Contributions to surface air temperature trends estimated from climate time series: Medium-term causalities

Cite as: Chaos **32**, 063128 (2022); https://doi.org/10.1063/5.0088042
Submitted: 12 February 2022 • Accepted: 01 June 2022 • Published Online: 17 June 2022

Igor I. Mokhov and Dmitry A. Smirnov

Contributions to surface air temperature trends estimated from climate time series: Medium-term causalities

Cite as: Chaos **32**, 063128 (2022); doi: 10.1063/5.0088042
Submitted: 12 February 2022 · Accepted: 1 June 2022 ·
Published Online: 17 June 2022

Igor I. Mokhov[1,2] and Dmitry A. Smirnov[1,3,a)]

AFFILIATIONS

[1]A.M. Obukhov Institute of Atmospheric Physics of the Russian Academy of Sciences, 3 Pyzhevsky Per., 119017 Moscow, Russia
[2]Department of Physics, Lomonosov Moscow State University, Leninskie Gory, 119991 Moscow, Russia
[3]Saratov Branch, Kotelnikov Institute of Radioengineering and Electronics of the Russian Academy of Sciences, 38 Zelyonaya Street, 410019 Saratov, Russia

Note: This article is part of the Focus Issue, Theory-informed and Data-driven Approaches to Advance Climate Sciences.
[a)]**Author to whom correspondence should be addressed:** smirnovda@yandex.ru

ABSTRACT

Contributions of various natural and anthropogenic factors to trends of surface air temperatures at different latitudes of the Northern and Southern hemispheres on various temporal horizons are estimated from climate data since the 19th century in empirical autoregressive models. Along with anthropogenic forcing, we assess the impact of several natural climate modes including Atlantic Multidecadal Oscillation, El-Nino/Southern Oscillation, Interdecadal Pacific Oscillation, Pacific Decadal Oscillation, and Antarctic Oscillation. On relatively short intervals of the length of two or three decades, contributions of climate variability modes are considerable and comparable to the contributions of greenhouse gases and even exceed the latter. On longer intervals of about half a century and greater, the contributions of greenhouse gases dominate at all latitudinal belts including polar, middle, and tropical ones.

Trends of the surface air temperatures on different spatial and temporal scales are determined by both the key natural modes of climate variability and the anthropogenic factor characterized by the changes of radiative forcing of greenhouse gases in the atmosphere. Currently, it is of great importance to reveal quantitative contributions of anthropogenic and natural factors at different latitudes of the Northern and Southern Hemispheres on various time intervals. Such contributions are estimated here from observational climate data with simplest empirical models using the concept of dynamical causal effect that quantifies a future (shorter-term or longer-term) response of one process to a change in an initial state or internal parameters of another process under all other equal conditions. Here, we change the behavior of a factor under study in an empirical autoregressive model (this is a change from an observed time series to a temporal constant equal to the starting value or the mean value of that time series) and examine the respective change of a linear trend of the temperature on any chosen time interval. The results are presented for the contributions of different factors on different time intervals (including the range from a couple of decades to half a century corresponding to medium-term dynamical causal effects) at different latitudinal belts: tropical, middle, and polar ones. These results evidence that the natural modes of climate variability contribute to the temperature trends sometimes as strongly as the greenhouse gases on the time intervals of about two or three decades but much weaker on intervals longer than half a century.

I. INTRODUCTION

Quantitative estimation of the role of natural and anthropogenic factors in the contemporary climate change is a key problem of the 21st century. An overall increase in the global surface air temperature (GST) revealed from observation data since the 19th century includes periods of its faster rise and periods of its decrease. In the beginning of the 21st century, the tendency of the global warming slowdown or "hiatus" has arisen. Still, the GST values in

the last years are among the highest ones in the entire observational dataset since the 19th century. With probability greater than 90%, more than a half of the GST rise since the middle of the 20th century is attributed to the anthropogenic rise of the atmospheric content of greenhouse gases (GHGs).[1]

The significant impact of the GHGs (especially CO_2) rise on the contemporary GST increase has been revealed from empirical data in many studies which take into account different natural factors including solar and volcanic activities, quasi-cyclic processes like El Nino/Southern Oscillation (ENSO), Atlantic Multidecadal Oscillation (AMO), and others; see, e.g., Refs. 1–32. In the time range of interest, natural variability, essentially, enhances or weakens the global warming via producing periods of faster warming and periods with almost no warming. In particular, Ref. 7 estimated the impacts of anthropogenic forcing, El Nino phenomena, solar activity, and volcanic activity that altogether explain up to three-quarters of temperature variance since the end of the 19th century. Those authors note that along with the dominating role of the anthropogenic factor, El Nino phenomena induce the GST changes up to 0.2 deg C on the time scales of several years, considerable volcanic eruptions—up to 0.3 deg C, and solar activity variations—about 0.1 deg C (see also Refs. 10 and 11). Many other works[2,3,8,11–13,18,19,21,23,26,27] confirmed the presence and statistical significance of the GHGs' impact on GST and compared it with the impact of other factors using different methods. However, along with such estimates of the impact of different factors on the global climate, it is necessary to obtain concrete numerical estimates of their contributions to temperature trends for different areas of the Earth from empirical data. In particular, Refs. 29 and 30 used a simple method based on trivariate autoregressive (AR) models, which is employed also in this work, and provided estimates of the contributions of GHGs and AMO to the GST trends and the trends of the temperatures at different latitudes of the Northern Hemisphere (NH). This work aims at estimating the contributions of a larger set of significant natural modes of climate variability (AMO, ENSO, Interdecadal Pacific Oscillation—IPO, Pacific Decadal Oscillation—PDO, and Antartic Oscillation—AAO also called Southern Annular Mode) along with GHGs at various latitudes of both NH and Southern Hemisphere (SH). Moreover, we address the question of how strongly the natural climate variability with time scales up to several decades can enhance or weaken warming at different latitudes on different time intervals, with a special attention to the intervals of about half a century and shorter. This is principally important, in particular, for the quantitative explanation of differences between the contemporary temperature trends at various NH and SH latitudes, including polar and subpolar latitudes with very different behaviors of the Arctic and Antarctic sea ice extents.[1,33] Indeed, apart from empirical estimates, climate models are able to reproduce many modes of climate variability, but not all significant modes of climate variability and their changes are modeled well enough.[34]

It is worth to note that the question under study is somewhat similar but still considerably different from detection and attribution of the climate change to one of the several selected factors addressed, e.g., in Refs. 35–46. In detection studies, *a priori* specified climate models (which are usually coupled atmosphere and ocean general circulation models) are used whose multiple realizations are generated under the control experiment condition, i.e., with a constant factor under consideration (e.g., constant atmospheric GHGs content if the impact of this factor is examined). The observed climate fields can be projected onto some typical model patterns called "fingerprints,"[35,37] which are often obtained from model climate change simulations and necessary to enhance detection capability (statistical power, "signal-to-noise" ratio)[35,37] of the method. If the scale factor (i.e., the corresponding component of the observed fields) significantly differs from control experiment values, one rejects the hypothesis of no impact of the factor under study whose change is included in climate change simulations (e.g., a certain scenario of the GHGs rise). In the attribution studies, several factors can be considered in turn with comparison of the observed data to model fields obtained in different climate change experiments, each including a change of only one factor. If only one of the experiments agrees well with observed data (after adjusting the scale factor), then the observed climate change is attributed to the impact of that factor. In those studies, one assumes that only one factor (or, more generally, a linear combination of them) contributes considerably to the observed climate change. All climate model parameters are not estimated from data and the entire model is supposed to be adequate. The climate field under study is supposed to be a linear combination of internal climate variability and the above patterns corresponding to climate change experiments, each with a single factor included. Under that setting, it is indeed difficult to assess numerically simultaneous contributions of different factors to temperature trends because it is difficult to carry out multiple climate change experiments with numerous possible linear combinations of different factors with different weights. On the other hand, if one studies the roles of different factors only in a coupled general circulation model, it is not an empirical estimation since the model parameters are not then estimated from data.

To avoid existing difficulties, one can try to assess the contributions to trends from different factors in a simple stochastic dynamical model whose parameters are estimated from the observed data. Probably, it is questionable whether such a model is adequate for the description of climate dynamics under different conditions, but the adequacy of the large general circulation models is also not completely assured. The advantage of a simple model is that it relies just on data and a simple form of the evolution equation without any assumptions concerning parameterizations, etc. Even if simple empirical models used here appear to be too simple in the future, it is reasonable to start purely empirical numerical estimation of simultaneous contributions of different factors to temperature trends with such models.

The method used here is based on stochastic dynamical models and aimed at causality estimation in line with such methods as phase-dynamic modeling,[46–55] linear and nonlinear Granger causality,[56–60] transfer entropies[61–72] and similar information-theoretic concepts,[73,74] convergent cross-mapping[75,76] and similar state space approaches,[77–79] cross-recurrence techniques,[80–82] spectral causalities,[83–88] and others.[89] Most of those methods describe short-term causalities, while the method used here assesses longer-term causal effects similarly to the idea of long-term causality that has been suggested in Refs. 12 and 13 and found its further development within the framework of dynamical causal effects.[90] The latter

concept includes short-term (transient) and long-term (asymptotic) effects of certain initial state or parameter interventions as presented in detail in Refs. 91–95 with a more general formulation in Ref. 96. The method used here is a particular case within that framework. It can be said to assess medium-term causal effects of parameter interventions into the behavior of various factors. From different viewpoints, intervention-based approaches have been developed and used also in Refs. 97–99 while causalities at different temporal scales have been considered in Refs. 100 and 101. A similar idea to account for the role of different external forcings based on empirical dynamical models was also implemented and applied to climate data studies in Refs. 102 and 103 continuing a series of works on empirical modeling from climate time series.[104–109]

Section II describes the climate data used for estimation, Sec. III presents the method, Sec. IV reports the results, and Sec. V concludes.

II. DATA UNDER ANALYSIS

Figure 1 presents the time series under study: interannual variations of the surface air temperature T at different latitudes of the NH and SH [Fig. 1(a)] and the indices of AMO, ENSO, IPO, PDO, and AAO with corresponding GHGs radiative forcing [Fig. 1(b)]. Temperature anomalies are given relatively to the reference period 1971–2000. We note deficiencies of the data for Antarctic latitudes, so the estimates for these latitudes presented below are of a more qualitative than a quantitative character. Selection of the above indices of the natural climate variability is determined by the attempt to include the long-term internal variability associated either with the Pacific Ocean (ENSO, IPO, PDO, and AAO) or with the Atlantic Ocean (AMO and NAO) into the empirical AR model for temperature variations. Only one of these indices at a time (except the NAO index) is included into the model along with the GHGs index to keep the model as simple as possible, representing both the anthropogenic factor and internal variability and retaining reasonable statistical properties. Taking into account, along with the AMO index, the NAO index with high interannual variability is not expected to reveal any significant contribution to temperature trends over several decades.

To represent surface air temperatures at various latitudes including the tropical (0°–30°N), middle (30°–60°N), and Arctic (60°–90°N) latitudes of the NH and the corresponding (0°–30°S, 30°–60°S, and 60°–90°S) latitudes of the SH, we have used the mean annual data since 1880 until now [Fig. 1(a)]. The data are the land–ocean temperatures from the Extended Reconstructed Sea Surface Temperature dataset (ERSST,[110,111] version 4) located at ftp://ftp.ncdc.noaa.gov/pub/data/noaaglobaltemp/operational/timeseries/ in the following six files (accessed on 08/16/2017): aravg.mon.land.60 N.90 N.v4.0.1.201706.txt, aravg.mon.land.30 N.60 N.v4.0.1.201706.txt, aravg.mon.land.00 N.30 N.v4.0.1.201706.txt, aravg.mon.land.30S.00 N.v4.0.1.201706.txt, aravg.mon.land.60S.30S.v4.0.1.201706.txt, and aravg.mon.land.90S.60S.v4.0.1.201706.txt (the dataset identifier is doi:10.7289/V5KD1VVF, the detailed description of the data is given at https://www.ncdc.noaa.gov/data-access/marineocean-data/extended-reconstructed-sea-surface-temperature-ersst-v4).

The anthropogenic influences are characterized by GHGs' radiative forcing over 1851–2012 with the main contribution from CO_2. The forcing dataset as used in GISS Climate Models[112] is located at https://data.giss.nasa.gov/modelforce/Miller_et_2014/Fi_Miller_et_al14_upd.txt (accessed on 10/10/2016).

Among the key modes of natural climate variability, we have used the index of AMO since 1856 (HadISST1 dataset).[113,114] Detrended AMO data are located at https://psl.noaa.gov/data/correlation//amon.us.long.data where the index is calculated north of 0°. For comparisons to previous results,[29,30] we have used the previous version of the index computed for the band 20°N–70°N [Fig. 1(b), cyan dashed line] located at http://www.esrl.noaa.gov/psd/data/correlation//amon.us.long.data (accessed on 05/04/2017, the detailed description of the data is given at https://psl.noaa.gov/data/timeseries/AMO/). The detrended AMO index possesses the characteristic period of about six decades. We have used different filters to focus on a slow component of the AMO index. As a representative case, the main results are shown here for the annual-mean data of the AMO index smoothed with a weighted moving average filter with 10-year window length and weights linearly decreasing with the time lag (i.e., the triangular temporal profile) down to zero at the lag of 11 years as in Ref. 91.

The strongest interannual variability of the global surface air temperature is associated with the El-Nino phenomena. We have used the ENSO index since 1870 until now (HadISST1 dataset),[114] which shows sea surface temperature anomalies in the region Nino-3,4 in the equatorial Pacific (5°S–5°N, 170–120°W) and is located at https://psl.noaa.gov/gcos_wgsp/Timeseries/Data/nino34.long.anom.data (accessed on 10/10/2016). Its plot is given in Fig. 1(b) with the blue line.

We have estimated also the contribution of the PDO and IPO to the surface temperature trends based on the HadISST1.1 dataset.[114] We have used the PDO index since 1854 until now based on NOAA's extended reconstruction of sea surface temperatures [ERSST Version 5 (https://www.ncdc.noaa.gov/teleconnections/pdo/, accessed on 10/26/2021)]. It is shown with the green line in Fig. 1(b). We have used the IPO index since 1870 until now. Indeed, along with the AMO, a considerable role in interdecadal climate variability is played by IPO, which is characterized by the TPI index (Tripole Index) defined as the difference between the sea surface temperature of the central equatorial Pacific (10°S–10°N, 170°E–90°W) and the mean sea surface temperature of the north-western (25°N–45°N, 140°E–145°W) and south-western (50°S–15°S, 150°E–160°W) Pacific.[115] The TPI index is shown with the black line in Fig. 1(b) and located at https://psl.noaa.gov/data/timeseries/IPOTPI/tpi.timeseries.hadisst1.1.data (accessed on 10/23/2020).

The additional index used is the AAO index for the period 1871–2012 (NOAA/NCEP Climate Prediction Center data).[116] The AAO is characterized by the difference of the standardized zonal mean sea level pressures between 40°S and 65°S. The AAO index is located at https://psl.noaa.gov/data/20thC_Rean/timeseries/monthly/SAM/sam.20crv2.long.data (accessed on 10/23/2020).

This work presents the analysis of the period since 1880 (the starting date of the temperature data) until 2012 (the ending date of the GHGs forcing and the AAO data). This period includes the data for each of the above variables.

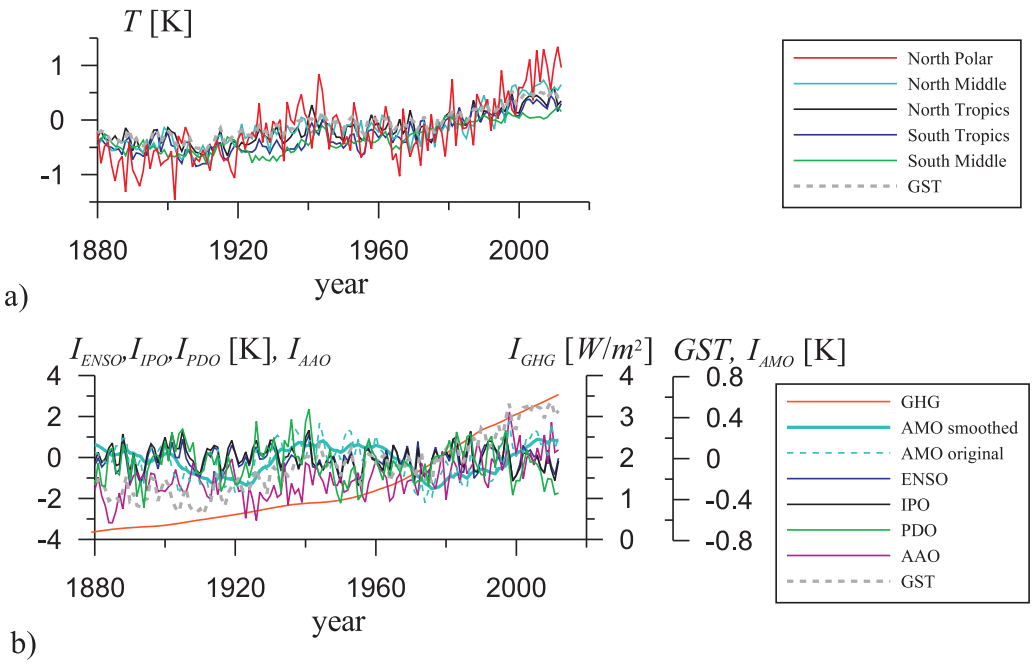

FIG. 1. Time series under analysis represent interannual variations of (a) surface air temperature T for the entire Earth (GST, gray dashes) and at various latitudes of the NH and the SH (the legend); (b) indices of AMO (filtered index is shown with the cyan solid line, unfiltered one with the cyan dashed line), ENSO (blue), IPO (black), PDO (green), and AAO (magenta) along with GHGs radiative forcing (brown).

III. METHOD OF DATA ANALYSIS

Contributions to temperature trends in each latitudinal zone are estimated on time intervals of the lengths ranging from 5 to 130 years with the aid of AR models analogously to Refs. 29 and 30. The approach fits to the framework of dynamical causal effects[13,90,91] based on the comparison of dynamics under alternative conditions. Under that approach, one considers a coupled stochastic (Markovian) dynamical system consisting of two subsystems X and Y which, in case of discrete time, reads

$$\begin{aligned} \mathbf{x}_n &= \mathbf{F}(\mathbf{x}_{n-1}, \mathbf{y}_{n-1}, \xi_{X,n}, \mathbf{a}_X, \mathbf{a}_{XY}), \\ \mathbf{y}_n &= \mathbf{G}(\mathbf{x}_{n-1}, \mathbf{y}_{n-1}, \xi_{Y,n}, \mathbf{a}_Y, \mathbf{a}_{YX}), \end{aligned} \tag{1}$$

where $\mathbf{x}$ and $\mathbf{y}$ are state vectors of arbitrary finite dimension, n is discrete time, (ξ_X, ξ_Y) is white noise, $\mathbf{a}_X$ and $\mathbf{a}_Y$ are vectors of individual parameters of subsystems X and Y, and $\mathbf{a}_{XY}$ and $\mathbf{a}_{YX}$ are vectors of coupling parameters in the respective directions. So, $\mathbf{a}_{XY} = 0$ means that the future dynamics of X is independent of any past and present states of Y, given the present state of X, and everything is the same for the opposite direction. To characterize an effect of coupling in the direction $Y \to X$, one performs some variation in the initial state or parameters of the subsystem Y and examines the response of the subsystem X at some future time instant or on some future time interval in an appropriate sense, which provides the corresponding dynamical causal effect. Here, the effect of interest is defined via variation of the parameter $\mathbf{a}_Y$ from any given value (corresponding to the observed dynamics) to such value that $\mathbf{G} = const$ (an appropriate parameterization of $\mathbf{G}$ is easily formulated), i.e., an alternative regime is a constant value of the vector $\mathbf{y}$. This is a kind of parameter intervention or parameter variation defined in Ref. 90. The response of X is here the change of the linear trend of a certain component x_i on some future time interval of moderate length. This is neither a very short-term effect (at time instants about one or several time steps ahead) nor a long-term effect (at time instants greater than any characteristic time scales of the entire system, i.e., close to an asymptotic effect). It is reasonable to call it a "medium-term effect," though strictly speaking this is a kind of a short-term effect as defined in Ref. 90. So, what we estimate below is the coupling characteristic of the type "parameter intervention—medium-term effect."

Specifically, we construct a model for each temperature anomaly T taking into account the influences of the GHGs and a natural variability mode I_M in the form

$$T_n = a_0 + a_1 T_{n-1} + a_2 I_{GHG,n-1} + a_3 I_{M,n-1} + \xi_n. \tag{2}$$

Here, n is discrete time (years), ξ_n is noise (residual errors of the model), I_{GHG} is GHGs radiative forcing, and I_M is the index of a climate mode. The evolution equations for I_{GHG} and I_M are not constructed and so are not explicitly shown in Eq. (2). The AR equation (2) is fitted to the entire observation interval via the ordinary least-squares technique, i.e., via minimization of the sum $S(\mathbf{a}) = \sum_n \xi_n^2$ of the squares of the residual errors $\xi_n = T_n - a_0 - a_1 T_{n-1} - a_2 I_{GHG,n-1} - a_3 I_{M,n-1}$ over the parameter vector $\mathbf{a}$. The index I_M is I_{AMO} (the above low-pass filtered AMO index) or I_{ENSO} (ENSO) or I_{IPO} (IPO) or I_{PDO} (PDO), or I_{AAO} (AAO). The

estimates of the coefficients a_0, a_1, a_2, a_3 are provided with the estimates of their standard errors (deviations) obtained automatically from the same regression estimation under the assumption of delta-correlated finite-variance noise ξ. They are computed as the mean squared prediction error multiplied by the inverse of A^TA where A is the matrix of regressors' values. The significance level at which the null hypothesis of a zero coefficient is rejected can be estimated via the inverse of the standard Gaussian cumulative distribution function evaluated at the estimated value of a coefficient divided by its estimated standard error.

To determine the contributions of anthropogenic and natural factors to linear temperature trends for each of the six latitudinal zones over a time interval $[L_{start}, L_{end}]$ with the length $L = L_{end} - L_{start}$, we analyzed time realizations of the AR model (2) with the estimated parameters $\hat{\mathbf{a}}$ in hypothetical regimes for natural variability modes or the GHGs atmospheric content: instead of the observed time series for a given factor (for example, a natural variability mode $I_{M,n}$, $n = 1880, \ldots, 2012$), we "fed" the model (2) with an artificially generated time series $\tilde{I}_{M,n}$ at its input. The initial value of T and the time series of another factor (in the above example, $I_{\mathrm{GHG},n}$, $n = 1880, \ldots, 2012$) at the model input were the actually observed values. The time series of the "external noise" ξ_n ($n = 1880, \ldots, 2012$) at the model input was the time series of the residual errors $\hat{\xi}_n$ corresponding to the minimum of their sum of squares. The contribution of each factor to the trend was estimated as the difference between the trends of the actually observed values T_n and the model values $\tilde{T}_n$ corresponding to the input signal $\tilde{I}_{M,n}$. This difference in the trends is equal to the linear trend of the temperature difference $\delta T_n = T_n - \tilde{T}_n$. In other words, we assume that the model (2) is equally applicable under the hypothetical condition of an alternative behavior of the factor under study. In this work, we take the hypothetical behavior to be a constant value $\tilde{I}_{M,n} = const$ (i.e., "absence of any dynamics" of I_M) after some starting time instant with unchanged behavior $\tilde{I}_{M,n} = I_{M,n}$ before that time instant. For any mode I_M, that constant level is just the empirical mean of I_M over the entire interval 1880–2012 and the starting time instant is the first instant n when the value $I_{M,n}$ gets approximately equal to that constant. For the factor I_{GHG}, the constant level is just I_{GHG} in the very beginning of the time series and so the starting time instant is 1880. Within the dynamical effects framework,[90] such hypothetical change of the factor under study in a model is a parameter intervention since the entire evolution operator of that factor is changed to another equation that reads $I_{M,n} = const$. Effects of that intervention are considered here on temporal horizons of the length of several decades.

The trend on each time interval $[L_{start}, L_{end}]$ (with L ranging from 5 to 130 years) was represented by a coefficient $\alpha_{\delta T}$ of the standard linear regression $\delta T_n = \alpha_{\delta T} n + \zeta_n$ obtained via the ordinary least-squares technique. In this way, we estimated the contributions to temperature trends from the five factors denoting such contributions as C_{GHG} (from GHGs), C_{AMO}(from AMO), C_{ENSO} (from ENSO), C_{IPO} (from IPO), and C_{AAO} (from AAO). We estimated also the actual trend of T, i.e., the coefficient α_T in the regression equation $T_n = \alpha_T n + \zeta_n$. To assess the relative role of each factor, we have used the corresponding ratios. Thus, such ratios are $C_{\mathrm{GHG}}/\alpha_T$, $C_{\mathrm{AMO}}/\alpha_T$, $C_{\mathrm{AMO}}/C_{\mathrm{GHG}}$, $\tilde{C}_{\mathrm{GHG}} = |C_{\mathrm{GHG}}|/(|C_{\mathrm{GHG}}| + |C_{\mathrm{AMO}}|)$, and $\tilde{C}_{\mathrm{AMO}} = |C_{\mathrm{AMO}}|/(|C_{\mathrm{GHG}}| + |C_{\mathrm{AMO}}|)$ for model (1) with GHGs and AMO. Everything is analogous for ENSO, IPO, PDO, and AAO instead of AMO.

Concerning the noise realization at the model input that is used to generate the hypothetical behavior, one could also use an ensemble of Gaussian white noise realizations similarly to Refs. 12 and 13. However, the basic idea here is to compare the model behavior under the change of a *single* factor and *other equal* conditions. So, if one studies a trend in a given time series, it should be compared to a trend in a corresponding alternative time series where noise realization (understood as a realization of external factors influencing the temperature) is one of the conditions to be held equal. If one studies a distribution of the trend values in various realizations of an empirical model, it is reasonable to compare a mean trend of that distribution to a mean trend of the distribution obtained for a hypothetical behavior of I_{GHG} or I_M. In our case, the trend estimate for an actually observed time series seems to be more interesting than some mean trend. A probabilistic context can be provided by checking the hypothetical behavior of the models with different AR parameters drawn from the Gaussian distribution with expectation equal to the least-squares parameter estimate and with the covariance matrix obtained from regression estimation as mentioned above. For each such trial model, one should consider its parameter values as "true" and obtain the corresponding noise realization as the residual errors ξ_n computed with those parameter values. Resulting ensembles of trend contribution estimates were computed for many models studied here. The relative standard deviation of those estimates appeared to equal the relative standard deviation of the respective AR coupling coefficient estimate (given in Table I). So, the generation of ensembles is not needed to estimate the uncertainties of the estimates of the contributions to trends.

This is the simplest method to estimate the contributions to the trends, which is based on a minimalistic empirical model. Hence, its advantages are the most reliable statistical estimates and the smallest number of assumptions. Surely, the unit-lag AR model (2) may not be the best one. Further studies with other models deserve efforts. In particular, we have used also linear AR models with greater time lags ranging up to 30 years and with higher AR orders ranging up to five in respect of each variable on the right-hand side of the AR equation. The optimal models turn out to correspond to quite considerable time lags of GHGs and AMO of more than 10 years. Their results concerning the estimates of the contributions to the temperature trends are overall similar to those presented here in terms of maximal values of the contributions over different time windows of a given length, while the timing of the maximum contribution (i.e., the location of the respective time window) differs from that for the unit-lag AR model. So, the conclusions about the values of the contributions to the trends are robust to such extension of the model structure. Still, reliability of such larger models deserves separate studies.

Multivariate linear AR models that include more factors may also be fitted instead of the trivariate models. For example, one can include all four natural variability modes under study and fit a 6-variate AR model. It may reduce a bias possibly induced by the choice of the simpler models (2). However, such a reduction in the bias may readily lead to an increase in the variance of parameter

TABLE I. Estimates of AR coefficients (rounded-off) with 95% intervals, Δa is the doubled standard error. The latitudinal zones are as follows: 1, Arctic; 2, middle latitudes of NH; 3, tropics of NH; 4, tropics of SH; 5, middle latitudes of SH; 6, Antarctic. Parentheses provide estimates of the significance level at which the hypothesis of the zero coefficient is rejected: bold font: at the level of $p < 0.05$ (highly significant); bold italic: at $0.05 < p < 0.1$; italic: at $0.1 < p < 0.2$; normal: non-significant; a_2 has the units of K/Wm^{-2}; a_3 is dimensionless except for AAO where it has units of K.

	Coefficients of the AR model (2) with the natural variability mode									
	AMO		ENSO		IPO		PDO		AAO	
Lat.	$a_2 \pm \Delta a_2$	$a_3 \pm \Delta a_3$	$a_2 \pm \Delta a_2$	$a_3 \pm \Delta a_3$	$a_2 \pm \Delta a_2$	$a_3 \pm \Delta a_3$	$a_2 \pm \Delta a_2$	$a_3 \pm \Delta a_3$	$a_2 \pm \Delta a_2$	$a_3 \pm \Delta a_3$
1	**0.35** ± 0.10 (<10^{-6})	**0.70** ± 0.50 (0.006)	**0.30** ± 0.10 (<10^{-6})	*0.09* ± 0.12 (0.13)	**0.31** ± 0.10 (<10^{-6})	*0.07* ± 0.11 (0.19)	**0.32** ± 0.10 (<10^{-6})	0.03 ± 0.07 (0.52)	**0.32** ± 0.11 (<10^{-6})	−0.02 ± 0.09 (0.74)
2	**0.21** ± 0.06 (<10^{-6})	**0.44** ± 0.25 (0.0005)	**0.16** ± 0.05 (<10^{-6})	0.03 ± 0.06 (0.35)	**0.16** ± 0.05 (<10^{-6})	0.02 ± 0.05 (0.54)	**0.16** ± 0.06 (<10^{-6})	0.01 ± 0.03 (0.73)	**0.15** ± 0.06 (<10^{-6})	0.01 ± 0.04 (0.59)
3	**0.15** ± 0.05 (<10^{-6})	**0.23** ± 0.20 (0.02)	**0.14** ± 0.05 (<10^{-6})	*0.04* ± 0.05 (0.16)	**0.14** ± 0.05 (<10^{-6})	0.02 ± 0.05 (0.36)	**0.13** ± 0.05 (<10^{-6})	−0.00 ± 0.03 (0.95)	**0.15** ± 0.05 (<10^{-6})	***−0.03*** ± 0.03 (0.06)
4	**0.17** ± 0.05 (<10^{-6})	0.07 ± 0.18 (0.43)	**0.18** ± 0.06 (<10^{-6})	*0.04* ± 0.05 (0.14)	**0.17** ± 0.06 (<10^{-6})	0.02 ± 0.05 (0.46)	**0.16** ± 0.05 (<10^{-6})	−0.00 ± 0.03 (0.78)	**0.17** ± 0.05 (<10^{-6})	−0.02 ± 0.03 (0.26)
5	**0.06** ± 0.03 (0.000 06)	0.00 ± 0.10 (0.96)	**0.06** ± 0.03 (0.000 06)	−0.00 ± 0.03 (0.78)	**0.06** ± 0.03 (0.000 06)	0.00 ± 0.02 (0.97)	**0.06** ± 0.03 (0.0001)	0.01 ± 0.02 (0.45)	**0.05** ± 0.03 (0.0005)	0.01 ± 0.02 (0.32)
6	**0.08** ± 0.07 (0.03)	−0.05 ± 0.50 (0.86)	**0.08** ± 0.07 (0.02)	***−0.11*** ± 0.12 (0.1)	**0.08** ± 0.07 (0.04)	−0.06 ± 0.12 (0.34)	**0.08** ± 0.07 (0.03)	−0.01 ± 0.07 (0.78)	**0.11** ± 0.09 (0.02)	−0.05 ± 0.10 (0.32)

estimates and so to a decrease in statistical significance of conclusions. Then, one will suspect that some parameter estimates in a 6-variate model are insignificant due to model overfitting and try to exclude the factors one by one to achieve the best model with appropriate corrections for multiple testing. It is still desirable to look carefully at all intermediate trial models and report all their characteristics that would make the text very long. We have preferred to start with simpler models and postpone a consideration of more complex models to future studies.

Similarly, accounting for nonlinearity with more general models (1) is also potentially significant. In particular, one could fit trivariate quadratic AR models instead of linear ones. However, such a model with a full polynomial includes 10 free parameters instead of the four parameters in the model (2). For a short time series at hand, it may readily lead again to a decrease in significance, i.e., to a bias reduction at the expense of an increase in variance. Besides, it is quite probable that nonlinear models will be only marginally better (if better at all) as it was the case in Ref. 10 with the analysis of the same data for the GST and solar activity; then, many polynomial terms will be superfluous and many model parameters will insignificantly differ from zero. Hence, a careful choice of the terms to be included into the nonlinear AR model may be necessary. Other forms of nonlinearity produce the respective questions concerning the model structure selection. Such studies are potentially useful and necessary but require long text to discuss each trial model in some detail and are less convenient as a first step.

So, the method with the simple model (2) in use seems to be the most reasonable as a first step among all methods based on the construction of dynamical models directly from empirical data without any presumed theoretical hypotheses about the climate processes under study.

Concerning the model consistency check that is regarded to be necessary for attribution,[38] all models (2) here agree well with the observed dynamics: The model residuals may be regarded as Gaussian white noise with reasonable accuracy (according to their autocorrelation function and histogram), and the ensembles of model time series obtained under different noise realizations cover the observed temperature time series quite well. Such analysis was done in Refs. 12 and 13 for similar AR models of GST with GHGs and solar and volcanic activity (instead of the modes of variability; still, the inclusion of those modes into the models here does not change the above model consistency conclusions). The difference from the consistency check of Ref. 38 is that the noise variance is estimated here from the data for each model separately, so each model agrees with the observed data up to its own variability level. Such flexibility of the model noise parameter is an advantage of the purely empirical approach used here, since the model variability in the attribution studies[38] is specified *a priori* and a model may be claimed there inconsistent only because its variability is too low, while it might be adequate if the variability level were adjusted.

IV. RESULTS

A. Empirical AR models

To estimate contributions of different factors to the temperature trends, we have fitted a trivariate AR model (2) with unit time lag for each surface air temperature anomaly T accounting for the

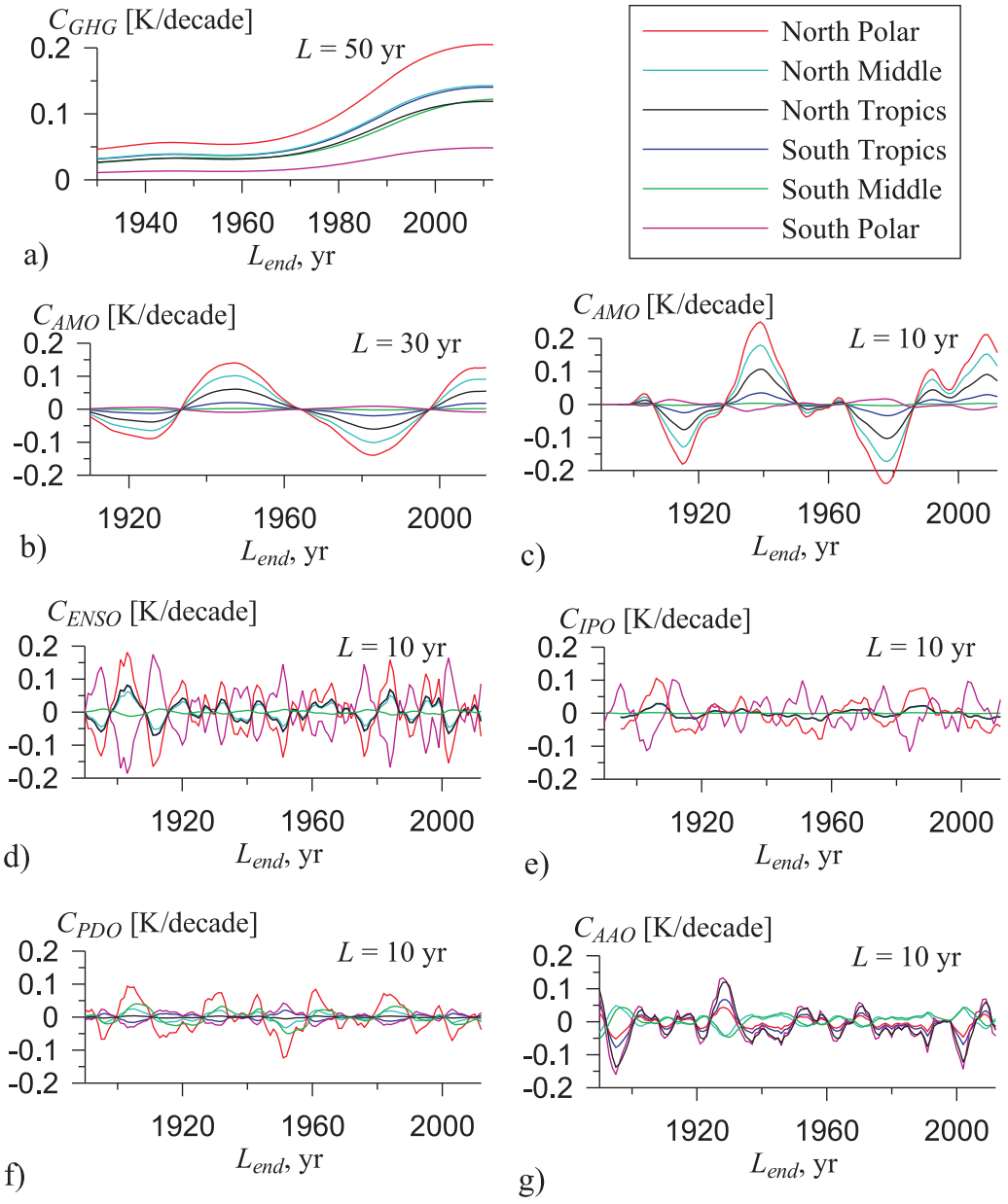

FIG. 2. Contributions of different factors to surface air temperature trends at various latitudes: (a) the contribution of the GHGs estimated in a 50-year moving window with a model (2) accounting for AMO, the estimates with models accounting for other natural modes are almost indistinguishable; (b) the contribution of AMO in a 30-year moving window; (c) that of AMO in a 10-year moving window; (d) that of ENSO in a 10-year moving window; (e) that of IPO in a 10-year moving window; (f) that of PDO in a 10-year moving window; and (g) that of AAO in a 10-year moving window.

impacts of GHGs and one of the natural variability modes. Table I presents estimates of the coefficients of the model (2) which characterize sensitivity of temperature anomalies at different latitudes to changes of the GHGs radiative forcing I_{GHG} and different indices I_M for the entire period under analysis (1880–2012). One can see from those coupling coefficients that the sensitivity to the GHGs changes is smallest for the middle latitudes of SH: it is 2.5 times as small (while a characteristic time is 2.5 times as large) as that for the tropics of NH. This is explained by the largest thermal inertia for the areas with higher percentage of the sea surface.

(1) **Thermal inertia.** An estimate of a characteristic time of temperature variations is obtained from the dimensionless coefficient a_1, which corresponds to a single time step equal here

TABLE II. Estimates of relative GHGs contributions C_{GHG}/α_T. Five numbers in each cell correspond to the models (2) accounting for AMO, ENSO, IPO, PDO, and AAO, respectively. Numbering of the latitudinal zones in the first column is the same as in Table I. The other four columns show the results for four different window lengths with the same window end point $L_{end} = 2012$.

Lat	20 years	30 years	50 years	130 years
1	0.33, 0.33, 0.34, 0.34, and 0.35	0.41, 0.42, 0.43, 0.42, and 0.43	0.64, 0.64, 0.66, 0.64, and 0.66	0.98, 0.98, 1.01, 0.99, and 1.02
2	0.41, 0.41, 0.42, 0.42, and 0.40	0.44, 0.45, 0.46, 0.45, and 0.43	0.68, 0.69, 0.70, 0.70, and 0.66	0.99,1.00, 1.01, 1.01, and 0.96
3	0.61, 0.61, 0.62, 0.61, and 0.71	0.71, 0.71, 0.72, 0.72, and 0.83	0.86, 0.86, 0.88, 0.87, and 1.00	0.98, 0.98, 1.00, 0.99, and 1.14
4	1.00, 0.99, 1.01, 0.72, and 1.07	1.22,1.21, 1.23, 0.68, and 1.32	0.95, 0.95, 0.96, 1.07, and 1.02	1.01,1.00, 1.02, 1.15, and 1.08
5	1.38, 1.38, 1.39, 1.40, and 1.26	1.86,1.86, 1.86, 1.88, and 1.70	1.15,1.16, 1.16, 1.16, and 1.06	1.02, 1.02, 1.02, 1.02, and 0.93
6	−0.52, −0.53, −0.49, −0.52, and −0.71	−0.68, −0.70, −0.65, −0.68, and −0.94	1.87,1.93, 1.77, 1.86, and 2.58	1.38,1.42, 1.30, 1.37, and 1.90

to 1 year. The less the value of a_1, the less inertial the process. The closer this coefficient to unity, the greater the relaxation time of the process that equals $\tau \approx 1/(1 - a_1)$ years. Naturally, inertia of a latitude band depends on the percentage of the sea surface. As mentioned above, the most inertial processes are those in the middle latitudes of SH where the relaxation time of the model (2) is estimated to be about 5 years. Just to compare, the mean relaxation time of the two tropical bands is about 1.7 years (1.8 years for the tropics of SH and 1.5 years for the tropics of NH). Thermal inertia of the middle latitudes of NH is characterized with the relaxation time of 1.4 years in the AR model (2) with AMO. The relaxation time for the polar bands is about 1.3 years. Estimates of the thermal inertia in the AR models (2) with different climatic modes somewhat differ from each other, but the middle latitudes of SH are the most inertial ones in any model.

(2) **Noise intensity estimates.** The variance σ^2 of the residual errors ξ_n characterizes intensity of the "noise," i.e., external inputs over intra-annual time scales. It is the least in the middle latitudes of SH ($0.08\ K^2$), three times as large in both tropical zones, five times as large at the middle latitudes of NH, and 25 times as large in both polar zones being slightly greater in Antarctic.

(3) **Coefficients of the coupling to GHGs.** According to the obtained estimates of the coupling coefficient a_2 (Table I), the impact of GHGs in all latitude bands is significant at the level of $p < 0.05$, i.e., the coefficient estimate exceeds twice its standard error estimate. Most often, the impact of GHGs appears to be far more significant, e.g., even for the middle latitudes of the SH in the model (2) with AAO, it is significant at $p = 0.0005$, i.e., the coefficient estimate is about 3.6 times as great as its standard error. The largest coupling coefficient $a_2 = 0.35$ K/(Wm^{-2}) is obtained for Arctic latitudes. This coefficient is about twice as small for the middle latitudes of the NH and for both tropical zones. It is somewhat greater in the tropics of the SH than in the tropics of the NH. As for the middle and polar latitudes of the SH, this coupling coefficient appears about five times as small as that for Arctic latitudes, being somewhat less in the middle latitudes than in the polar ones.

(4) **Coefficients of the coupling to AMO.** According to the estimates of the dimensionless coefficient a_3 (Table I), the impact of AMO for the entire period under analysis is essential only in the NH. It is the strongest one at Arctic latitudes reaching the value of 0.7 significantly nonzero at $p = 0.005$. This coefficient is 1.5 times as small at the middle latitudes of the NH and three times as small at the tropical latitudes of the NH. According to this coefficient, the impact of AMO at the tropical latitudes of SH is 10 times weaker than that in Arctic. The coefficient a_3 for the tropics of SH is not significant even at the level of 0.2. So, it is reasonable to consider the contribution of AMO only to the temperature trends in the NH because the relative error of the trend estimate obtained with the model (2) is very close to the relative error of the corresponding coupling coefficient as was also confirmed in our numerical experiments.

(5) **Coefficients of the coupling to ENSO.** According to the estimates of the coefficient a_3 (Table I), the impact of ENSO is strongest at polar latitudes, its difference from zero is

TABLE III. Estimates of the relative contributions of AMO, ENSO, IPO, PDO, and AAO. Each estimate is reported for four window lengths (20, 30, 50, and 130 years) with the same window end point $L_{end} = 2012$. Numbering of the latitude zones in the first column is the same as in Table I. Bold font highlights the values exceeding 0.1 K/decade with the corresponding AR coefficient a_3 significant at the level of $p < 0.2$ or at a smaller p (italic shows such values for larger p, i.e., with the insignificant AR coefficient a_3).

	C_{AMO}/α_T				C_{ENSO}/α_T				C_{IPO}/α_T				C_{PDO}/α_T				C_{AAO}/α_T			
Lat.	20	30	50	130	20	30	50	130	20	30	50	130	20	30	50	130	20	30	50	130
1	**0.33**	**0.28**	**0.11**	0.03	**−0.10**	−0.03	−0.00	0.01	**−0.11**	−0.06	0.00	−0.02	−0.06	−0.05	−0.00	−0.00	−0.02	−0.02	−0.03	−0.03
2	**0.42**	**0.31**	**0.12**	0.03	−0.06	−0.02	0.00	0.01	−0.06	−0.03	0.00	−0.01	−0.03	−0.02	−0.00	−0.00	0.04	0.03	0.04	0.04
3	**0.45**	**0.36**	**0.10**	0.02	**−0.13**	−0.04	0.00	0.01	−0.09	−0.05	0.00	−0.01	−0.01	−0.01	−0.00	−0.00	**−0.19**	**−0.18**	**−0.18**	**−0.14**
4	0.20	0.17	0.03	0.01	**−0.18**	−0.06	0.00	0.01	*−0.12*	−0.08	0.00	−0.01	0.03	0.03	0.00	0.00	*−0.15*	*−0.14*	−0.09	−0.07
5	0.03	0.03	0.00	0.00	0.04	0.01	−0.00	−0.00	−0.01	−0.01	0.00	−0.00	*−0.19*	*−0.16*	0.01	−0.00	*0.20*	*0.25*	*0.12*	0.08
6	*0.14*	*0.13*	−0.09	−0.01	**−0.67**	**−0.25**	0.02	−0.05	*−0.49*	*−0.31*	−0.01	*0.10*	*−0.13*	*−0.12*	0.01	0.01	*0.44*	*0.40*	*−0.98*	*−0.50*

significant at $p = 0.1$ (for Antarctic) and $p = 0.13$ (for Arctic). At Antarctic latitudes, the coupling coefficient to ENSO possesses an opposite sign (negative) in comparison to other latitudes. It is essential that for both tropical zones, this coefficient is two or three times as small. There, it is also less significant with $p = 0.14$ or 0.16. It is even less and non-significant in the middle latitudes of both hemispheres. Thus, ENSO affects only the tropical and polar zones.

(6) **Coefficients of the coupling to IPO.** According to the estimates of the coefficient a_3 (Table I), the impact of IPO is about twice as small as that of ENSO. The most significant estimate of a_3 is obtained for Arctic ($p = 0.19$). Thus, the impact of IPO is most clearly (but still very weakly) seen in the Arctic zone.

(7) **Coefficients of the coupling to PDO.** The estimates of this coefficient a_3 are not significant at all latitudes as reported in Table I.

(8) **Coefficients of the coupling to AAO.** According to the estimates of the coefficient a_3 (Table I), the impact of AAO is most significant at tropical latitudes of NH ($p = 0.06$), even more significant than that of ENSO. This coefficient is non-significant at all other latitudes. Still, one can note that it is negative for both tropical zones, where the coupling coefficients from ENSO and IPO are positive. Thus, according to the AAO as a representative of the Pacific Ocean, the latter affects considerably only the temperature variations in the tropical latitudes of the NH.

B. Contributions of various factors to the temperature trends

Contributions of the GHGs to the trends were estimated in time windows of the lengths ranging from 10 to 130 years. Figure 2(a) presents those contributions estimated in a moving window of length of 50 years. To estimate them, the observed values of a temperature are compared to corresponding model values obtained under the condition of constant GHGs radiative forcing at the level of 1880 year (see Section III). The largest values of the GHGs contribution to the trends are obtained for Arctic latitudes: they equal about 0.2 K/decade and even greater in the last decades. The smallest values are obtained for Antarctic latitudes. For the middle latitudes of NH and tropical latitudes of SH, the maximal values of the GHGs' contribution are about 0.15 K/decade, while they are somewhat less for the tropical latitudes of NH and the middle latitudes of SH. Relative values of the GHGs contribution to the trends at various latitudes differ between the time windows.

The contributions of several climatic modes (AMO, ENSO, IPO, PDO, and AAO) are presented in Fig. 2 for moving windows of the lengths of 30 [Fig. 2(b)] and 10 years [Figs. 2(c)–2(g)]. The largest values are achieved by the contributions to temperature trends at Arctic latitudes, up to 0.2 K/decade and sometimes even greater. The results of a more detailed analysis for last decades based on the fixed-end time windows ($L_{end} = 2012$ year) with a moving start point are given in Tables II–IV. Table II presents the GHGs contribution to the trends C_{GHG} divided by the angular coefficient of the trend α_T itself (see Section III) at different latitudes for the models (2) accounting for four natural modes. The ratios C_{GHG}/α_T are less than 0.5 only for the relatively short time windows (2–3 decades or shorter) and only at extratropical latitudes. On the time scales

TABLE IV. Contributions of natural variability modes relative to GHGs contribution $\tilde{C}_{AMO}$, $\tilde{C}_{ENSO}$, $\tilde{C}_{IPO}$, $\tilde{C}_{PDO}$, and $\tilde{C}_{AAO}$. Each value is given for four different window lengths with the same window end point $L_{end} = 2012$. Numbering of the latitude zones in the first column is the same as in Table I. Bold font highlights the values exceeding 0.1 with the corresponding AR coefficient a_3 significant at the level of $p < 0.2$ or at a smaller p (italic shows such values for larger p, i.e., with the insignificant AR coefficient a_3).

	AMO				ENSO				IPO				PDO				AAO			
Lat.	20	30	50	130	20	30	50	130	20	30	50	130	20	30	50	130	20	30	50	130
1	**0.50**	**0.40**	**0.11**	0.03	**0.23**	0.08	0.00	0.01	**0.24**	**0.13**	0.00	0.02	*0.14*	*0.11*	0.00	0.00	0.06	0.04	0.04	0.03
2	**0.51**	**0.41**	**0.12**	0.03	*0.12*	0.04	0.00	0.01	*0.11*	0.07	0.00	0.01	0.06	0.04	0.00	0.00	0.09	0.07	0.06	0.04
3	**0.42**	**0.34**	**0.10**	0.02	**0.18**	0.06	0.00	0.01	*0.13*	0.07	0.00	0.01	0.01	0.01	0.00	0.00	**0.21**	**0.18**	**0.15**	**0.11**
4	*0.17*	*0.12*	0.03	0.01	**0.16**	0.05	0.00	0.01	*0.11*	0.06	0.00	0.01	0.04	0.04	0.00	0.00	*0.12*	*0.10*	0.08	0.06
5	0.02	0.02	0.00	0.00	0.03	0.01	0.00	0.00	0.01	0.00	0.00	0.00	*0.12*	0.08	0.00	0.00	*0.14*	*0.13*	0.10	0.07
6	*0.22*	*0.16*	0.05	0.01	**0.56**	**0.27**	0.01	0.03	*0.50*	*0.32*	0.01	0.07	*0.20*	*0.15*	*0.01*	*0.01*	*0.38*	*0.30*	*0.28*	*0.21*

longer than half a century, the GHGs contribution dominates at all latitudes.

Table III presents the contributions of the four climatic modes relative to the trends themselves at various latitudes. The ratios C_{AMO}/α_T, C_{ENSO}/α_T, C_{IPO}/α_T, C_{PDO}/α_T, and C_{AAO}/α_T do not exceed 0.5 for various time intervals at various latitudes except for Antarctic with non-representative long-term data. The most essential contributions of climatic modes are seen over relatively short time intervals, about 2–3 decades and shorter. Maximal values of relative contributions are obtained for AMO at various latitudes of NH. A considerable relative contribution of AAO occurs at the middle latitudes of SH, though it is almost statistically insignificant as discussed above (Table I).

Table IV presents the contributions of the four modes relative to the GHGs' contribution, i.e., the ratios $\tilde{C}_{AMO} = |C_{AMO}|/(|C_{GHG}| + |C_{AMO}|)$ etc. These ratios are the largest for relatively short time intervals as well. In particular, the values of $\tilde{C}_{AMO}$ are maximal in NH where they reach 0.5 at the middle and polar latitudes for 20-year time intervals. For SH, the values of $\tilde{C}_{AMO}$ are considerably smaller. The trend contributions of ENSO are most significant not only at the tropical latitudes, but also at the polar ones. At polar latitudes, considerable trend contributions of IPO are also revealed. Considerable trend contributions of AAO in SH are seen not only on the time scales of about two or three decades, but also on the scale of half a century, though their statistical significance is negligible as discussed above (Table I).

V. CONCLUSIONS

According to the presented results, the contributions of the key modes of natural variability to the surface air temperature trends on relatively short time intervals within three decades reach and can exceed (in absolute value) ±0.2 K/decade, while they are not considerable as compared to the contribution of the GHGs' atmospheric content rise on time intervals about half a century and longer. The GHGs' contribution always increases, reaching 0.2 K/decade in the last two decades and even somewhat exceeding this value. The GHGs contribution dominates on time intervals of about half a century and longer and sometimes even on shorter intervals. The estimates of the contribution to trends were done here via assessing medium-term causal effects in empirical autoregressive models according to the dynamical effects framework.[90] Validity of these estimates and conclusions is essentially based on the accuracy of the available empirical data and the validity of the model form (2), which includes the relevance of the set of potentially influencing factors (i.e., I_{GHG} and various I_M) selected for the analysis. The results in this work are obtained with minimal assumptions about the data used and the empirical dynamic models that characterize the Earth's climate system. Such assessments require further comprehensive testing of the role of data quality and the modeling approaches used.

These estimates are especially important to compare the contemporary trends of surface air temperatures at various latitudes of NH and SH with the assessment of the relative roles of the key natural variability modes on different temporal horizons. In particular, an overall increase in the Antarctic sea ice extent in the last few decades (up to the last years) according to the satellite data (available only starting from 1970s) accompanied with the global warming and a fast decrease in the Arctic sea ice extent is related to the general decrease in the surface temperature at sub-Antarctic latitudes, which occurred since 1970s until 2016 when a fast decrease in the sea ice extent in the Southern Ocean was noticed. This is related to regional manifestations of natural climate oscillations with periods up to several decades accompanied by the global century-scale warming and a relatively weak temperature trend over the ocean in SH. The cross-correlation and the cross-wavelet analyses evidence a significant coherence and a negative correlation between the surface temperature and the sea ice extent in the last few decades both in Arctic and Antarctic (see, e.g., Ref. 33). According to the estimates obtained in this work, a contribution of AAO, in particular, to the surface temperature trends at different latitudes of SH and tropical latitudes of NH is seen not only on the time scales of 20–30 years, but also on the time scales of half a century and longer. It should be taken into account in constructing future projections of regional climate changes on the basis of climate models. It is necessary for such models to describe adequately the natural climate variability and its contribution to the regional temperature trends on various temporal horizons. Currently, many important modes of climate variability are reproduced by such models, but there are also modes of variability that are not simulated well enough (e.g., Ref. 34).

ACKNOWLEDGMENTS

This study was supported by the Ministry of Science and Higher Education of the Russian Federation (Agreement No.

075-15-2021-577 with A.M. Obukhov Institute of Atmospheric Physics RAS) using the results of the analysis of climate variability features at different latitudes obtained within the framework of the Russian Science Foundation Project No. 19-17-00240.

AUTHOR DECLARATIONS

Conflict of Interest

The authors have no conflicts to disclose.

Author Contributions

Igor I. Mokhov: Conceptualization (lead); Formal analysis (supporting); Investigation (equal); Methodology (equal); Writing – original draft (equal). **Dmitry A. Smirnov:** Conceptualization (supporting); Formal analysis (lead); Investigation (equal); Methodology (equal); Writing – original draft (equal).

DATA AVAILABILITY

The data that support the findings of this study are available from the corresponding author upon reasonable request.

REFERENCES

[1]N. L. Bindoff, P. A. Stott, K. M. AchutaRao, M. Allen, N. Gillett, D. Gutzler, K. Hansingo, G. Hegerl, Y. Hu, S. Jain, I. I. Mokhov, J. Overland, J. Perlwitz, R. Sebbari, X. Zhang *et al.*, "Ch. 10," in *Climate Change 2013: The Physical Science Basis*, edited by T. F. Stocker (IPCC, Cambridge University Press, 2013).
[2]R. S. J. Tol and A. F. de Vos, Theor. Appl. Climatol. **48**, 63 (1993).
[3]R. K. Kaufmann and D. I. Stern, Nature **388**, 39 (1997).
[4]B. D. Santer, T. M. L. Wigley, C. Doutriaux, J. S. Boyle, J. E. Hansen, P. D. Jones, G. A. Meehl, E. Roeckner, S. Sengupta, and K. E. Taylor, J. Geophys. Res. **106**(D22), 28033, https://doi.org/10.1029/2000JD000189 (2001).
[5]M. R. Allen, N. P. Gillett, J. A. Kettleborough, G. Hegerl, R. Schnur, P. A. Stott, G. Boer, C. Covey, T. L. Delworth, G. S. Jones, J. F. B. Mitchell, and T. P. Barnett, Surv. Geophys. **27**, 491 (2006).
[6]R. Kaufmann, H. Kauppi, and J. Stock, Clim. Change **77**, 249 (2006).
[7]P. F. Verdes, Phys. Rev. Lett. **99**, 048501 (2007).
[8]J. L. Lean and D. H. Rind, Geophys. Res. Lett. **35**, L18701, https://doi.org/10.1029/2008GL034864 (2008).
[9]M. Lockwood and P. Roy, Soc. A Math. Phys. **464**, 1387 (2008).
[10]I. I. Mokhov and D. A. Smirnov, Izv., Atmos. Oceanic Phys. **44**, 263, https://doi.org/10.1134/S0001433808030018 (2008).
[11]J. L. Lean and D. H. Rind, Geophys. Res. Lett. **36**, L15708, https://doi.org/10.1029/2009GL038932 (2009).
[12]I. I. Mokhov and D. A. Smirnov, Dokl. Earth Sci. **427**, 798 (2009).
[13]D. A. Smirnov and I. I. Mokhov, Phys. Rev. E **80**, 016208 (2009).
[14]G. Foster and S. Rahmstorf, Environ. Res. Lett. **6**, 044022 (2011).
[15]G. Kopp and J. Lean, Geophys. Res. Lett. **38**, L01706, https://doi.org/10.1029/2010GL045777 (2011).
[16]R. Kaufmann, H. Kauppi, M. Mann, and J. Stock, Proc. Natl. Acad. Sci. U.S.A. **108**, 11790 (2011).
[17]C. Loehle and N. Scafetta, Open. Atmos. Sci. J. **5**, 74 (2011); available at https://benthamopen.com/contents/pdf/TOASCJ/TOASCJ-5-74.pdf.
[18]A. Attanasio and U. Triacca, Theor. Appl. Climatol. **103**, 103 (2011).
[19]E. Kodra, S. Chatterjee, and A. R. Ganguly, Theor. Appl. Climatol. **104**, 325 (2011).
[20]G. V. Gruza and E. Y. Rankova, *Observed and Expected Climate Changes Over Russia: Surface and Temperature* (RIHMI-WDC, Obninsk, 2012) (in Russian).
[21]I. I. Mokhov, D. A. Smirnov, and A. A. Karpenko, Dokl. Earth Sci. **443**, 381 (2012).
[22]J. Imbers, A. Lopez, C. Huntingford, and M. R. Allen, J. Geophys. Res. Atmos. **118**, 3192, https://doi.org/10.1002/jgrd.50296 (2013).
[23]U. Triacca, A. Attanasio, and A. Pasini, Environmetrics **24**, 260 (2013).
[24]J. Zhou and K. K. Tung, J. Atmos. Sci. **70**, 3 (2013).
[25]D. I. Stern and R. K. Kaufmann, Clim. Change **122**, 257 (2014).
[26]I. I. Mokhov and D. A. Smirnov, Dokl. Earth Sci. **467**, 384 (2016).
[27]A. Stips, D. Macias, C. Coughlan, E. Garcia-Gorriz, and X. S. Liang, Sci. Rep. **6**, 21691 (2016).
[28]M. B. Stolpe, I. Medhaug, and R. Knutti, J. Climate **30**, 6279 (2017).
[29]I. I. Mokhov and D. A. Smirnov, Dokl. Earth Sci. **480**, 602 (2018).
[30]I. I. Mokhov and D. A. Smirnov, Russ. Meteorol. Hydrol. **43**, 557 (2018).
[31]J. B. Kajtar, M. Collins, L. M. Frankcombe, M. H. England, T. J. Osborn, and M. Juniper, Geophys. Res. Lett. **46**, 2232, https://doi.org/10.1029/2018GL081462 (2019).
[32]L. A. McBride, A. P. Hope, T. P. Canty, B. F. Bennett, W. R. Tribett, and R. J. Salawitch, Earth Syst. Dyn. **12**, 545 (2021).
[33]I. I. Mokhov and M. R. Parfenova, Dokl. Earth Sci. **496**, 66 (2021).
[34]G. Flato, J. Marotzke, B. Abiodun, P. Braconnot, S. C. Chou, W. Collins, P. Cox, F. Driouech, S. Emori, V. Eyring, C. Forest, P. Gleckler, E. Guilyardi, C. Jakob, V. Kattsov, C. Reason, M. Rummukainen *et al.*, "Ch. 9," in *Climate Change 2013: The Physical Science Basis*, edited by T. F. Stocker (IPCC, Cambridge University Press, 2013).
[35]K. Hasselmann, J. Climate **6**, 1957 (1993).
[36]G. C. Hegerl, H. von Storch, K. Hasselmann, B. D. Santer, U. Cubasch, and P. D. Jones, J. Climate **9**, 2281 (1996).
[37]K. Hasselmann, Clim. Dyn. **13**, 601 (1997).
[38]M. R. Allen and S. F. B. Tett, Clim. Dyn. **15**, 419 (1999).
[39]M. R. Allen and P. A. Stott, Clim. Dyn. **21**, 477 (2003).
[40]C. Huntingford, P. A. Stott, M. R. Allen, and F. H. Lambert, Geophys. Res. Lett. **33**, L05710, https://doi.org/10.1029/2005GL024831 (2006).
[41]A. Ribes, J.-M. Azais, and S. Planton, Clim. Dyn. **33**, 707 (2009).
[42]G. C. Hegerl and F. Zwiers, WIREs Clim. Change **2**, 570 (2011).
[43]L. Jia and T. DelSole, J. Clim. **25**, 7122 (2012).
[44]A. Ribes and L. Terray, Clim. Dyn. **41**, 2837 (2013).
[45]J. Imbers, A. Lopez, C. Huntingford, and M. R. Allen, J. Clim. **27**, 3477 (2014).
[46]T. DelSole, L. Trenary, X. Yan, and M. K. Tippett, Clim. Dyn. **52**, 4111 (2019).
[47]M. G. Rosenblum and A. S. Pikovsky, Phys. Rev. E **64**, 045202(R) (2001).
[48]M. Paluš and A. Stefanovska, Phys. Rev. E **67**, 055201(R) (2003).
[49]D. A. Smirnov and B. P. Bezruchko, Phys. Rev. E **68**, 046209 (2003).
[50]D. Smirnov, B. Schelter, M. Winterhalder, and J. Timmer, Chaos **17**, 013111 (2007).
[51]M. Timme, Phys. Rev. Lett. **98**, 224101 (2007).
[52]I. T. Tokuda, S. Jain, I. Z. Kiss, and J. L. Hudson, Phys. Rev. Lett. **99**, 064101 (2007).
[53]B. Kralemann, L. Cimponeriu, M. Rosenblum, A. Pikovsky, and R. Mrowka, Phys. Rev. E **76**, 055201 (2007).
[54]D. A. Smirnov and B. P. Bezruchko, Phys. Rev. E **79**, 046204 (2009).
[55]Z. Levnajić and A. Pikovsky, Phys. Rev. Lett. **107**, 034101 (2011).
[56]C. W. J. Granger, Econometrica **37**, 424 (1969).
[57]D. Marinazzo, M. Pellicoro, and S. Stramaglia, Phys. Rev. Lett. **100**, 144103 (2008).
[58]I. Vlachos and D. Kugiumtzis, Phys. Rev. E **82**, 016207 (2010).
[59]L. Faes, G. Nollo, and A. Porta, Phys. Rev. E **83**, 051112 (2011).
[60]B. Wahl, U. Feudel, J. Hlinka, M. Wächter, J. Peinke, and J. A. Freund, Phys. Rev. E **93**, 022213 (2016).
[61]T. Schreiber, Phys. Rev. Lett. **85**, 461 (2000).
[62]M. Palus, V. Komarek, Z. Hrncir, and K. Sterbova, Phys. Rev. E **63**, 046211 (2001).
[63]K. Hlavackova-Schindler, M. Palus, M. Vejmelka, and J. Bhattacharya, Phys. Rep. **441**, 1 (2007).
[64]A. Bahraminasab, F. Ghasemi, A. Stefanovska, P. V. E. McClintock, and H. Kantz, Phys. Rev. Lett. **100**, 084101 (2008).
[65]M. Staniek and K. Lehnertz, Phys. Rev. Lett. **100**, 158101 (2008).
[66]J. T. Lizier and M. Prokopenko, Eur. Phys. J. B **73**, 605 (2010).
[67]J. Runge, J. Heitzig, V. Petoukhov, and J. Kurths, Phys. Rev. Lett. **108**, 258701 (2012).

[68]J. Sun and E. M. Bollt, Physica D **267**, 49 (2014).
[69]M. Wibral, R. Vicente, and J. T. Lizier, *Directed Information Measures in Neuroscience* (Springer, Berlin, 2014).
[70]J. Runge, Phys. Rev. E **92**, 062829 (2015).
[71]J. Runge, V. Petoukhov, J. F. Donges, J. Hlinka, N. Jajcay, M. Vejmelka, D. Hartman, N. Marwan, M. Paluš, and J. Kurths, Nat. Commun. **6**, 8502 (2015).
[72]T. Bossomaier, L. Barnett, M. Harre, and J. T. Lizier, *An Introduction to Transfer Entropy: Information Flow in Complex Systems* (Springer, Switzerland, 2016).
[73]X. S. Liang and R. Kleeman, Phys. Rev. Lett. **95**, 244101 (2005).
[74]X. S. Liang, Phys. Rev. E **94**, 052201 (2016).
[75]G. Sugihara, R. May, H. Ye, C. Hsieh, E. Deyle, M. Fogarty, and S. Munch, Science **338**, 496 (2012).
[76]D. Harnack, E. Laminsky, M. Schuenemann, and K. P. Pawelzik, Phys. Rev. Lett. **119**, 098301 (2017).
[77]J. Arnhold, K. Lehnertz, P. Grassberger, and C. E. Elger, Physica D **134**, 419 (1999).
[78]D. Chicharro and R. G. Andrzejak, Phys. Rev. E **80**, 026217 (2009).
[79]R. G. Andrzejak and T. Kreuz, Europhys. Lett. **96**, 50012 (2011).
[80]M. C. Romano, M. Thiel, J. Kurths, and C. Grebogi, Phys. Rev E **76**, 036211 (2007).
[81]J. F. Donges, Y. Zou, N. Marwan, and J. Kurths, Europhys. Lett. **87**, 48007 (2009).
[82]J. H. Feldhoff, R. V. Donner, J. F. Donges, N. Marwan, and J. Kurths, Phys. Lett. A **376**, 3504 (2012).
[83]M. Kaminski, M. Ding, W. A. Truccolo, and S. L. Bressler, Biol. Cybern. **85**, 145 (2001).
[84]L. Baccala and K. Sameshima, Biol. Cybern. **84**, 463 (2001).
[85]A. Brovelli, M. Ding, A. Ledberg, Y. Chen, R. Nakamura, and S. L. Bressler, Proc. Natl. Acad. Sci. U.S.A. **101**, 9849 (2004).
[86]B. Schelter, M. Winterhalder, M. Eichler, M. Peifer, B. Hellwig, B. Guschlbauer, C. H. Lucking, R. Dahlhaus, and J. Timmer, J. Neurosci. Methods **152**, 210 (2006).
[87]M. Dhamala, G. Rangarajan, and M. Ding, Phys. Rev. Lett. **100**, 018701 (2008).
[88]P. A. Stokes and P. L. Purdon, Proc. Natl. Acad. Sci. U.S.A. **114**, 7063 (2017).
[89]J. Prusseit and K. Lehnertz, Phys. Rev. E **77**, 041914 (2008).
[90]D. A. Smirnov, Phys. Rev. E **90**, 062921 (2014).
[91]D. A. Smirnov and I. I. Mokhov, Phys. Rev. E **92**, 042138 (2015).
[92]D. A. Smirnov, Chaos **28**, 075303 (2018).
[93]D. A. Smirnov, Europhys. Lett. **128**, 20006 (2019).
[94]D. A. Smirnov, Phys. Rev. E **102**, 062139 (2020).
[95]D. A. Smirnov, Chaos **31**, 073127 (2021).
[96]D. A. Smirnov, Phys. Rev. E **105**, 034209 (2022).
[97]N. Ay and D. Polani, Adv. Complex Syst. **11**, 17 (2008).
[98]M. Baldovin, F. Cecconi, and A. Vulpiani, Phys. Rev. Res. **2**, 043436 (2020).
[99]A. Auconi, B. M. Friedrich, and A. Giansanti, Europhys. Lett. **135**, 28002 (2021).
[100]M. Palus, Phys. Rev. Lett. **112**, 078702 (2014).
[101]L. Faes, G. Nollo, S. Stramaglia, and D. Marinazzo, Phys. Rev. E **96**, 042150 (2017).
[102]D. Mukhin, A. Gavrilov, E. Loskutov, J. Kurths, and A. Feigin, Sci. Rep. **9**, 7328 (2019).
[103]D. Mukhin, A. Gavrilov, A. Seleznev, and M. Buyanova, Geophys. Res. Lett. **48**, e2020GL091287, https://doi.org/10.1029/2020GL091287 (2020).
[104]D. Mukhin, A. Gavrilov, A. Feigin, E. Loskutov, and J. Kurths, Sci. Rep. **5**, 15510 (2015).
[105]D. Mukhin, E. Loskutov, A. Mukhina, A. Feigin, I. Zaliapin, and M. Ghil, J. Clim. **28**, 1940 (2015).
[106]D. Mukhin, D. Kondrashov, E. Loskutov, A. Gavrilov, A. Feigin, and M. Ghil, J. Clim. **28**, 1962 (2015).
[107]D. Mukhin, A. Gavrilov, E. Loskutov, A. Feigin, and J. Kurths, Clim. Dyn. **51**, 2301 (2018).
[108]A. Gavrilov, A. Seleznev, D. Mukhin, E. Loskutov, A. Feigin, and J. Kurths, Clim. Dyn. **52**, 2199 (2019).
[109]A. Gavrilov, S. Kravtsov, and D. Mukhin, Chaos **30**, 123110 (2020).
[110]B. Huang, V. F. Banzon, E. Freeman, J. Lawrimore, W. Liu, T. C. Peterson, T. M. Smith, P. W. Thorne, S. D. Woodruff, and H.-M. Zhang, J. Clim. **28**, 911 (2015).
[111]W. Liu, B. Huang, P. W. Thorne, V. F. Banzon, H.-M. Zhang, E. Freeman, J. Lawrimore, T. C. Peterson, T. M. Smith, and S. D. Woodruff, J. Clim. **28**, 931 (2015).
[112]R. L. Miller, G. A. Schmidt, L. S. Nazarenko, N. Tausnev, S. E. Bauer, A. D. Del Genio, M. Kelley, K. K. Lo, R. Ruedy, D. T. Shindell, I. Aleinov, M. Bauer, R. Bleck, V. Canuto, Y.-H. Chen, Y. Cheng, T. L. Clune, G. Faluvegi, J. E. Hansen, R. J. Healy, N. Y. Kiang, D. Koch, A. A. Lacis, A. N. LeGrande, J. Lerner, S. Menon, V. Oinas, C. Pérez García-Pando, J. P. Perlwitz, M. J. Puma, D. Rind, A. Romanou, G. L. Russell, M. Sato, S. Sun, K. Tsigaridis, N. Unger, A. Voulgarakis, M.-S. Yao, and J. Zhang, J. Adv. Model. Earth Syst. **6**, 441 (2014).
[113]D. B. Enfield, A. M. Mestas-Nunez, and P. J. Trimble, Geophys. Res. Lett. **28**, 2077, https://doi.org/10.1029/2000GL012745 (2001).
[114]N. A. Rayner, D. E. Parker, E. B. Horton, C. K. Folland, L. V. Alexander, D. P. Rowell, E. C. Kent, and A. Kaplan, J. Geophys. Res. **108**(D14), 4407, https://doi.org/10.1029/2002JD002670 (2003).
[115]B. J. Henley, J. Gergis, D. J. Karoly, S. B. Power, J. Kennedy, and C. K. Folland, Clim. Dyn. **45**, 3077 (2015).
[116]D. Gong and S. Wang, Geophys. Res. Lett. **26**, 459, https://doi.org/10.1029/1999GL900003 (1999).